Subtle design changes control the difference in colour reflection from the dorsal and ventral wing-membrane surfaces of the damselfly *Matronoides cyaneipennis*

M.R. Nixon,[1,*] A.G. Orr[2] and P. Vukusic[1]

[1]*School of Physics, University of Exeter, EX4 4QL, UK*
[2]*School of the Environment, Griffith University, Nathan, Q4111, Australia*
[*]*M.R.Nixon@exeter.ac.uk*

Abstract: The hind wings of males of the damselfly *Matronoides cyaneipennis* exhibit iridescence that is blue dorsally and green ventrally. These structures are used semiotically in agonistic and courtship display. Transmission electron microscopy reveals these colours are due to two near-identical 5-layer distributed Bragg reflectors, one placed either side of the wing membrane. Interestingly the thicknesses of corresponding layers in each distributed Bragg reflector are very similar for all but the second layer from each outer surface. This one key difference creates the significant disparity between the reflected spectra from the distributed Bragg reflectors and the observed colours of either side of the wing. Modelling indicates that modifications to the thickness of this layer alone create a greater change in the peak reflected wavelength than is observed for similar modifications to the thickness of any other layer. This results in an optimised and highly effective pair of semiotic reflector systems, based on extremely comparable design parameters, with relatively low material and biomechanical costs.

OCIS codes: (310.4165) Multilayer design; (240.0310) Thin films; (310.1620) Interference coatings; (310.6188) Spectral properties.

References and links

1. M. F. Land, "The physics and biology of animal reflectors," Prog. Biophys. Mol. Biol. **24**, 75–106 (1972).
2. D. L. Fox, *Animal Biochromes and Structural Colours* (University of California Press, 1976).
3. P. Vukusic and J. R. Sambles, "Photonic structures in Biology," Nature **424**(6950), 852–855 (2003).
4. J. P. Vigneron, M. Rassart, Z. Vértesy, K. Kertész, M. Sarrazin, L. P. Biró, D. Ertz, and V. Lousse, "Optical structure and function of the white filamentary hair covering the edelweiss bracts," Phys. Rev. E Stat. Nonlin. Soft Matter Phys. **71**(1), 011906 (2005).
5. B. J. Glover and H. M. Whitney, "Structural colour and iridescence in plants: the poorly studied relations of pigment colour," Ann. Bot. (Lond.) **105**(4), 505–511 (2010).
6. E. Denton, "Reflectors in fishes," Sci. Am. **224**(1), 64–72 (1971).
7. J. Zi, X. Yu, Y. Li, X. Hu, C. Xu, X. Wang, X. Liu, and R. Fu, "Coloration strategies in peacock feathers," Proc. Natl. Acad. Sci. U.S.A. **100**(22), 12576–12578 (2003).
8. T. Trzeciak and P. Vukusic, "Photonic crystal fiber in the polychaete work *Pherusa* sp," Phys. Rev. E Stat. Nonlin. Soft Matter Phys. **80**(6), 061908 (2009).
9. D. G. Stavenga, H. L. Leertouwer, N. J. Marshall, and D. Osorio, "Dramatic colour changes in a bird of paradise caused by uniquely structured breast feather barbules," Proc. Biol. Sci. **278**(1715), 2098–2104 (2011).
10. J. A. Noyes, P. Vukusic, and I. R. Hooper, "Experimental method for reliably establishing the refractive index of buprestid beetle exocuticle," Opt. Express **15**(7), 4351–4358 (2007).
11. A. E. Seago, P. Brady, J. P. Vigneron, and T. D. Schultz, "Gold bugs and beyond: a review of iridescence and structural colour mechanisms in beetles (Coleoptera)," J. R. Soc. Interface **6**(Suppl 2), S165–S184 (2009).
12. P. Vukusic, J. R. Sambles, C. R. Lawrence, and R. J. Wootton, "Quantified interference and diffraction in single *Morpho* butterfly scales," Proc. Biol. Sci. **266**(1427), 1403–1411 (1999).

#179627 - $15.00 USD Received 12 Nov 2012; revised 13 Dec 2012; accepted 17 Dec 2012; published 14 Jan 2013

13. S. Yoshioka and S. Kinoshita, "Single-scale spectroscopy of structurally colored butterflies: measurements of quantified reflectance and transmittance," J. Opt. Soc. Am. A **23**(1), 134–141 (2006).
14. J. W. Galusha, L. R. Richey, J. S. Gardner, J. N. Cha, and M. H. Bartl, "Discovery of a diamond-based photonic crystal structure in beetle scales," Phys. Rev. E Stat. Nonlin. Soft Matter Phys. **77**(5), 050904 (2008).
15. C. Pouya, D. G. Stavenga, and P. Vukusic, "Discovery of ordered and quasi-ordered photonic crystal structures in the scales of the beetle *Eupholus magnificus*," Opt. Express **19**(12), 11355–11364 (2011).
16. B. D. Wilts, K. Michielsen, J. Kuipers, H. De Raedt, and D. G. Stavenga, "Brilliant camouflage: photonic crystals in the diamond weevil, *Entimus imperialis*," Proc. Biol. Sci. **279**(1738), 2524–2530 (2012).
17. K. Michielsen and D. G. Stavenga, "Gyroid cuticular structures in butterfly wing scales: biological photonic crystals," J. R. Soc. Interface **5**(18), 85–94 (2008).
18. L. Poladian, S. Wickham, K. Lee, and M. C. J. Large, "Iridescence from photonic crystals and its suppression in butterfly scales," J. R. Soc. Interface **6**(Suppl 2), S233–S242 (2009).
19. P. Vukusic, R. J. Wootton, and J. R. Sambles, "Remarkable iridescence in the hindwings of the damselfly *Neurobasis chinensis chinensis (*Linnaeus) (Zygoptera: Calopterygidae)," Proc. Biol. Sci. **271**(1539), 595–601 (2004).
20. R. O. Prum, J. A. Cole, and R. H. Torres, "Blue integumentary structural colours in dragonflies (Odonata) are not produced by incoherent Tyndall scattering," J. Exp. Biol. **207**(22), 3999–4009 (2004).
21. T. Hariyama, M. Hironaka, and D. G. Stavenga, "The Leaf Beetle, the Jewel Beetle and the Damselfly; Insects with a Multilayered Show Case," In *Structural colour in biological systems - principles and applications*, S. Kinoshita and S. Yoshioka eds. (Osaka University Press, Osaka, Japan, 2005).
22. J.-H. Dirks and D. Taylor, "Veins Improve Fracture Toughness of Insect Wings," PLoS ONE **7**(8), e43411 (2012).
23. S. N. Gorb, A. Kesel, and J. Berger, "Microsculpture of the wing surface in Odonata: evidence for cuticular wax covering," Arthropod Struct. Dev. **29**(2), 129–135 (2000).
24. I. R. Hooper, P. Vukusic, and R. J. Wootton, "Detailed optical study of the transparent wing membranes of the dragonfly *Aeshna cyanea*," Opt. Express **14**(11), 4891–4897 (2006).
25. R. J. Wootton, "Functional morphology of insect wings," Annu. Rev. Entomol. **37**(1), 113–1140 (1992).
26. A.G. Orr and M. Hämäläinen, *The metalwing demoiselles of the eastern tropics: their identification and biology*, (Natural History Publications, Borneo, 2007).
27. P. Vukusic and D. G. Stavenga, "Physical methods for investigating structural colours in biological systems," J. R. Soc. Interface **6**(Suppl 2), S133–S148 (2009).
28. P. Vukusic, R. Sambles, C. R. Lawrence, and G. Wakely, "Sculpted-multilayer optical effects in two species of Papilio butterfly," Appl. Opt. **40**(7), 1116–1125 (2001).
29. P. Vukusic, J. R. Sambles, and C. R. Lawrence, "Structurally assisted blackness in butterfly scales," Proc. Biol. Sci. **271**(Suppl 4), S237–S239 (2004).
30. D. G. Stavenga, B. D. Wilts, H. L. Leertouwer, and T. Hariyama, "Polarized iridescence of the multi-layered elytra of the Japanese jewel beetle, *Chrysochroa fulgidissima*," Philos. Trans. R. Soc. London, Ser. B **366**(1565), 709–723 (2011).
31. D. G. Stavenga, H. L. Leertouwer, T. Hariyama, H. A. De Raedt, and B. D. Wilts, "Sexual dichromatism of the damselfly *Calopteryx japonica* caused by a melanin-chitin multilayer in the male wing veins," PLoS ONE **7**(11), e49743 (2012).
32. H. L. Leertouwer, B. D. Wilts, and D. G. Stavenga, "Refractive index and dispersion of butterfly chitin and bird keratin measured by polarizing interference microscopy," Opt. Express **19**(24), 24061–24066 (2011).
33. S. Yoshioka and S. Kinoshita, "Direct determination of the refractive index of natural multilayer systems," Phys. Rev. E Stat. Nonlin. Soft Matter Phys. **83**(5), 051917 (2011).
34. H. J. Dumont, J. R. Vanfleteren, J. F. De Jonckheere, and P. H. H Weekers, "Phylogenetic relationships, divergence time estimation, and global biogeographic patterns of calopterygoid damselflies (Odonata, Zygoptera) inferred from ribosomal DNA sequences," Syst. Biol. **54**(3), 347–362 (2005).
35. A. Günther, "Reproductive behavior of *Neurobasis kaupi* (Odonata: Calopterygidae)," Int. J. Odonat. **9**(2), 151–164 (2006).
36. A. G. Orr, "Territorial and courtship displays in Bornean Chlorocyphidae (Zygotptera)," Odonatologica **25**, 119–141 (1996).

1. Introduction

Many biological systems are known to use periodic variations in refractive index on the sub-micron scale to produce a range of optical effects [1–3]. The resulting structural colouration has been documented in many species of both flora [4, 5] and fauna [6–9]. In particular, insects have been shown to possess a diverse array of photonic structures: bright metallic colours from various beetles' continuous multilayer (also referred to as distributed Bragg reflector, or DBR) structures [10, 11], striking blue from the discrete multilayer (DBR) structures present in many species of *Morpho* butterflies [12, 13] and coloured reflection from 3D periodic structures in weevils [14–16] and also in some butterflies [17, 18]

#179627 - $15.00 USD Received 12 Nov 2012; revised 13 Dec 2012; accepted 17 Dec 2012; published 14 Jan 2013

Some species of Odonata exhibit a range of bright structural colours in their wing membranes and bodies [19–21]. The montane, stream-dwelling Bornean damselfly *Matronoides cyaneipennis* is particularly interesting as the dorsal and ventral sides of its hind wing membrane reflect different colours. Both fore- and hind wings' upper surfaces are deep blue, as is the lower surface of the hind wing; that of the forewing, however, is deep green. The forewing is similarly coloured on its upper surface, but the underside reflects the same deep blue colour as on the dorsum of both wings.

In *M. cyaneipennis* the wing membrane is divided into small partitions known as cells [22] (not to be confused with eukaryotic cells), most of which are approximately 400 μm x 200 μm, each framed by a particularly dense network of rigid veins – a type of structure that is typical of odonatan wings [23, 24]. The major longitudinal veins are known to contribute towards both mechanical support and the transmission of haemolymph, oxygen and sensory information, while the numerous fine cross-veins strengthen the wing, preventing tearing of the membrane [25]. The individual cells are set at differing angles over the wing surface. This affects gross reflective properties and produces an overall fractured scintillating effect, rather than a continuous sheet of colour.

The iridescent wing colours of *M. cyaneipennis* and related species have a semiotic function in both agonistic displays between males and in courtship. In this species the upperside colour is displayed most conspicuously in agonistic displays whereas the underside colours are displayed during courtship [26]. We investigated the origin of the distinctly different colour-reflectance properties from either side of the wing membrane and present a detailed analysis of the observed structures and the colour-appearance they produce.

2. Methods

2.1 Animals

Male specimens of *M. cyaneipennis* were collected under permit from the Silau Silau stream at an altitude of 1400 m in Mt Kinabalu National Park, Sabah, Malaysia. The wings were removed from the body so they could be mounted flat for optical microscope imaging and reflectance spectrometry. Small regions of the hind wing were also removed and prepared for transmission electron microscopy (TEM).

2.2 Imaging

Individual wings of *M. cyaneipennis* were imaged optically using a Zeiss Axiocam MRc5 connected to a Zeiss Axioscope 2 optical microscope. Small wing-regions and individual cells were imaged under epi-illumination in bright and dark fields. TEM of the wings was undertaken after fixing samples in 3% glutaraldehyde at 21 °C for 2 h followed by rinsing in sodium cacodylate buffer. Subsequent fixing in 1% osmic acid in buffer for 1 h was followed by block staining in 2% aqueous uranyl acetate for 1 h, dehydration through an ethanol series (ending with 100% ethanol) and embedding in Taab resin. After ultra-microtoming, sample sections were stained with lead citrate and examined using a JEOL 100S TEM instrument. In addition scanning electron microscopy (SEM) was undertaken with a Nova 600 NanoLab Dualbeam system, after sputter-coating the samples with 5 nm of gold palladium.

2.3 Reflectance spectrometry

Small sections of the wings were fixed to a sample mount that was attached to a micromanipulator capable of a several-micron adjustment resolution in x, y and z positioning and one-degree resolution in polar and azimuthal angle orientation. This allowed accurate positioning of the sample, ensuring that the centre of the cell under investigation was co-incident with the centre of the illuminating beam-spot.

An Ocean Optics HPX-2000 high power xenon light-source was used to illuminate the sample at chosen angles from 20 to 50 degrees. An appropriate series of lenses was used to

#179627 - $15.00 USD Received 12 Nov 2012; revised 13 Dec 2012; accepted 17 Dec 2012; published 14 Jan 2013

focus the beam-spot to a diameter of approximately 100 µm. Reflected light was captured using a series of collecting lenses and delivered to an optical fibre that was connected to an Ocean Optics HR2000 + high-resolution spectrometer.

Normal incidence reflectance spectra were unobtainable with this method. They were collected using conventional microspectrophotometry (MSP) techniques [27]. Spectra were taken from many sample regions (approximately 15 µm in diameter) to account for the colour-variation associated with sampling only small regions which can be attributed to small variations in the properties of the underlying structure.

2.4 Analysis of wing structures and optical modelling

A large number of TEM images from different regions across the hindwing were analysed using ImageJ (http://rsbweb.nih.gov/ij/). The layer thicknesses of the DBR systems identified in these images were measured in two ways; firstly by considering the layers as discrete 1D blocks (block method) and secondly by considering the pixel-intensity variation across a line running normal to these layers' surfaces (profile method). Predicted reflectance spectra were produced using a Fresnel-based code written and run in MATLAB (http://www.mathworks.com).

3. Results and Analysis

Figure 1 shows the colour-appearance of two cells from the same region of *M. cyaneipennis'* hindwing; demonstrating the blue of the dorsal surface (Fig. 1(a)) and contrasting green of the ventral surface (Fig. 1(b)).

Optical reflectance data from the dorsal and ventral surfaces, from within single-cell membrane regions (typical beam-spot diameter of 150 µm), are presented in Fig. 2. There is a blue-shift of reflectance maxima with increasing angle of incidence that is characteristic of distributed Bragg reflectors (DBRs). At near-normal incidence (measured via MSP) the dorsal and ventral DBRs exhibit maxima at approximately 480 nm and 545 nm respectively. This decreases to approximately 440 nm and 480 nm respectively at 50 degrees, with a typical reduction in peak intensity.

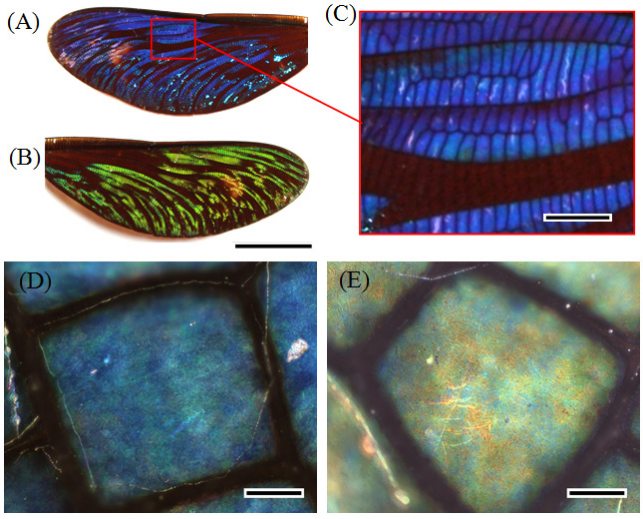

Fig. 1. Optical microscope images of the surfaces of the hind wings of *M. cyaneipennis*. (A) Low-magnification image of the dorsal side of the wing, (B) low-mag image of the ventral side of the wing, (C) close-up taken from image in (A), (D) high-magnification image of a dorsal cell, (E) high-mag image of a ventral cell. Scale bars are 10mm (A and B), 2mm (C), 100 µm (D) and 200 µm (E).

#179627 - $15.00 USD Received 12 Nov 2012; revised 13 Dec 2012; accepted 17 Dec 2012; published 14 Jan 2013

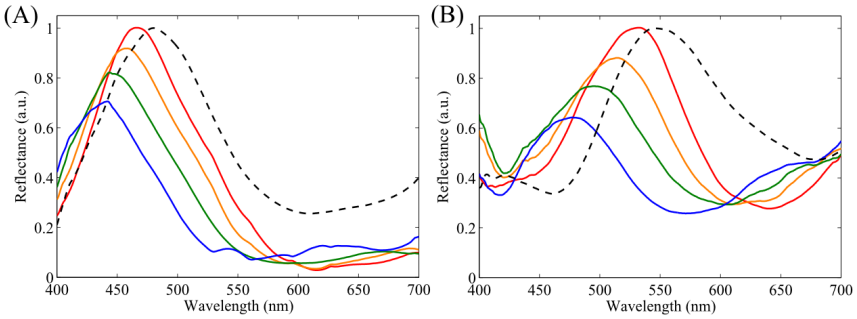

Fig. 2. Measured reflections from (A) the dorsal side and (B) the ventral side of the wing membrane at a range of incident angles; 20 degrees (red), 30 degrees (orange), 40 degrees (green) and 50 degrees (blue). Near-normal incidence reflectance, measured using MSP is represented by the black-dashed data. (Near-normal incidence data and 20 degree incidence data are both normalised to 100% reflectance; other data scales correctly relative to the 20 degree data).

The TEM images of *M. cyaneipennis* reveal the presence of layering within the wing cell membrane (Fig. 3). This layering forms the DBRs that generate the wing colour. It comprises two DBR structures, one dorsal and the other ventral, separated by a thick dark-contrasted layer that is almost half the total thickness of the whole wing membrane. Both DBRs appear to comprise five layers of different thicknesses. Visual and software-based analyses of the differences between dorsal and ventral DBRs reveal very similar thicknesses between all but one corresponding dorsal and ventral layer. There is a much more distinct and optically significant difference between the thicknesses of the corresponding second-outermost layers in each DBR. The second layer in the dorsal DBR is typically 20 per cent thinner than the second layer in the ventral DBR.

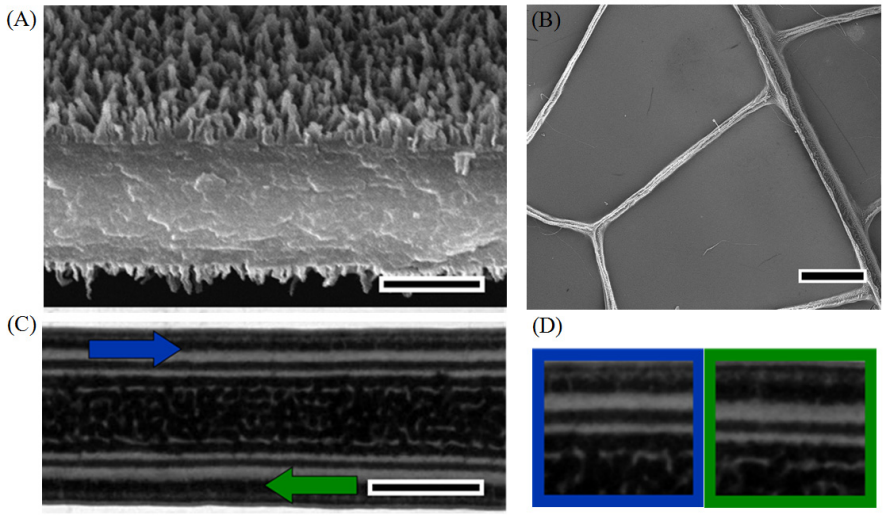

Fig. 3. (A) SEM image showing a fractured edge of wing cell membrane from *M. cyaneipennis*. (B) SEM image showing several cells on the wing membrane. (C) TEM image showing a cross-section of the structurally coloured cell membrane from the hindwing of *M. cyaneipennis* revealing the layered structures present on either side of the central thick dark-contrasted layer that form the dorsal and ventral DBRs. (D) Side-by side comparison of magnified sections of the TEM image shown in (C). The positions of the regions highlighted by the blue and green coloured boxes in (D) are indicated by the blue and green arrows in (C). Specifically, however, the blue and green arrow tips point along the second layer in each DBR. [Scale bars 1 µm (A), 75 µm (B), 1 µm (C)].

#179627 - $15.00 USD Received 12 Nov 2012; revised 13 Dec 2012; accepted 17 Dec 2012; published 14 Jan 2013

The TEM stains used during preparation have resulted in electron opacity contrast between alternating sets of layers. This generates the grayscale contrast of the TEM image. As has been described elsewhere in relation to TEM stains used in biophotonic systems [9, 28], this indicates not only the different refractive indices of the dark and light contrasted layers, but also different amounts of optical absorption (represented by the imaginary component of the complex refractive index). The dark contrasted layers are strongly associated with the presence of melanin.

The central thick layer is extremely dark-contrasted, but with some fine aperiodic light-contrasted structure within it. While the mechanism for the growth of fine structure of this form is unclear, but possibly related to the presence of melanin in granular form, its presence does offer the potential for an enhanced optical absorption cross-section within this layer. This stems from the random scattering that arises due to the associated geometrically aperiodic refractive index mismatches. It results in increased path length within the absorbing region, an effect that has been measured in an analogous system within highly absorbing butterfly scales [29].

Theoretical appreciation of the differences between the dorsal and ventral DBRs in relation to the large contrast in the thickness of only the second outermost layer can be developed through modelling. To this end we used thin-film modelling methods to determine whether this five-layer DBR is particularly sensitive to thickness changes in the second outermost layer.

3.1 Modelling of the DBRs

When dealing with DBR systems, models are usually created based on the assumption that the layers within the system have infinitesimally thin interface boundaries. These models are subsequently created with discrete changes in refractive index between layers. The edges of individual layers within the DBR structures of *M. cyaneipennis*, however, are not so clearly defined in spatial terms. This could be said to apply also to other biophotonic systems. The change of material between neighbouring layers occurs over a boundary plane that is not necessarily narrow in comparison to the layer thicknesses. Physically this infers a gradual change in refractive index between layers, rather than a step-change. One way of accessing this more realistic and continuous refractive index profile across biological multilayers is by taking a pixel-intensity line-plot across the DBR structures identified in TEM images and scaling the resulting profile between suitable maximum and minimum refractive index values. This is shown in Fig. 4(a) for *M. cyaneipennis'* DBR system. It is an approach that has been described previously by Stavenga *et al.* for some other biophotonic systems [30].

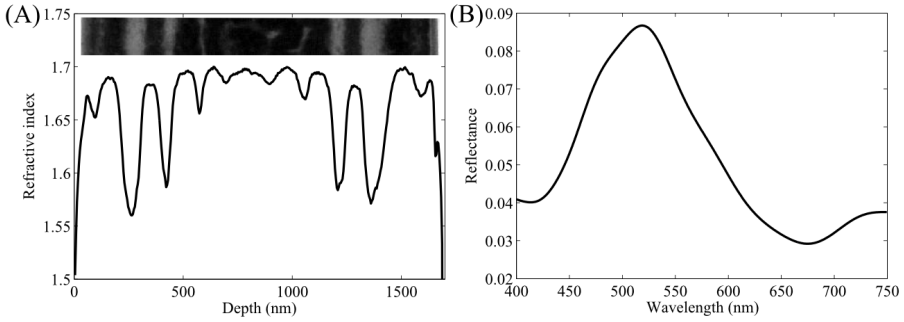

Fig. 4. (A) Measured refractive index profile (from a strip of width 100 nm) across a TEM of *M. cyaneipennis'* cross-sectional structure (the TEM from which the intensity profile is taken is shown in the insert). The intensity profile shown is the pixel-intensity average across the 100 nm width of the TEM. (B) Theoretically modelled reflectance of the *M. cyaneipennis* system using the refractive index profile shown in (A).

#179627 - $15.00 USD Received 12 Nov 2012; revised 13 Dec 2012; accepted 17 Dec 2012; published 14 Jan 2013

Modelling DBR systems in such a way that includes this profile-based gradual change in refractive index between layers, namely, using pixel-intensity changes across TEM images, is in many ways a more realistic representation of the actual refractive index profile of the DBR system. For example, Fig. 4(b) presents the theoretical wavelength-dependent reflectance associated with the refractive index profile shown in Fig. 4(a). On its own, this reflectance appears qualitatively at least, representative of the experimental spectra collected from the wing cell and shown in Fig. 2(a). However, variations in intra-TEM and especially inter-TEM layer dimensions lead to significant challenges when it comes to calculating reflectances based on layer thickness averages. Such variations in layer thicknesses, from one local position to the next, are extremely common in biophotonic systems. They form a "biological noise", of sorts, resulting from complex biochemical processes involved in the growth dynamics of the structures. In particular with *M. cyaneipennis,* this form of layer thickness variation is especially evident. So much so, that TEMs of cross-sections from adjacent regions of intra-cell wing membrane display significant variation in the thickness of equivalent layers and lead to the local intra-cell colour variation of the membrane that is evident in Figs. 1(a) and 1(b). This results in pixel-intensity profiles of TEMs, taken from neighbouring one-micron diameter regions of the same cell that do not overlie one another. This difficulty is demonstrated in Fig. 5(a) where two separate intensity line plots have been averaged to form a single intensity line-plot. The two TEM cross-section structures are aligned at the same surface position at the left side (blue DBR side) of the profile. Small thickness and intensity variations across even the first few layers leads to a reduction in the integrity of the DBR's profile when the two are averaged. This affects the modelled reflection significantly in relation to peak wavelength and intensity (shown in Fig. 5(b)).

Creating an average pixel-intensity line-plot using separate line-plots, or creating line-plots using one extended TEM sample-width, can have similar associated problems. A different approach to the profile method may be required for the analysis of structures which display significant inter-TEM variation in their pixel intensity (refractive index) profiles. The same applies when any subsequent optimisation of the DBR system is needed.

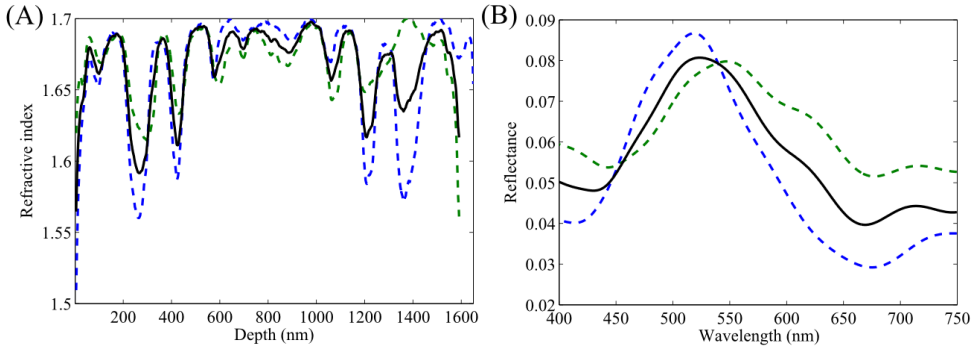

Fig. 5. (A) Assigned refractive index profiles across two different TEM images, both taken from the same intra-cell wing-membrane region, taken using the pixel-intensity profile method. Blue and green dashed lines represent refractive index profiles across each TEM (TEM strip width = 100 nm); black solid line represents the average of the two individual TEM profiles. (B) Theoretical data showing the contrasting reflectance spectra of the two intra-cell membrane regions, that correspond to the refractive index profiles shown in (A).

Theoretical models based on representing pixel-intensity variations across DBRs in TEMs as discrete step-changes in refractive index enables the measurement of individual layers' thicknesses, and their variations, to be made over several TEM images. These may then be averaged to simulate the colour-mixing effect of the small juxtaposed colour regions that arise due to the layer thickness variations across the cell's membrane. Another advantage

#179627 - $15.00 USD Received 12 Nov 2012; revised 13 Dec 2012; accepted 17 Dec 2012; published 14 Jan 2013

of taking this block approach is that it easily enables individual layer parameters to be investigated in more detail than is possible with the profile method.

For the *M. cyaneipennis* wing membrane structure, we created a theoretical model based on the average of several hundred thickness measurements of each layer over many TEM images. The refractive index parameters of this model were refined so that the system's theoretical modelled reflectance matched its experimentally measured reflectance. The specifics of this practice are well documented [27]. The associated complex refractive indices of both dark and light contrasted layers were determined using this method (shown in Table 1): their values are consistent with other measurements of iridescent odonate wing membrane refractive indices [21, 24, 31]. The real (n) and imaginary (k) components of the refractive indices of insect cuticle are known to exhibit some dispersion. Measurements of the extent of this dispersion in n and/or in k have been described in several investigations [12, 31–33]. For the modelling of the experimental data presented here, however, the extent of this refractive index dispersion does not make a significant difference to the wing membrane's reflection peak position, shape and intensity since, over the small wavelength range of the reflection maxima, the extent of dispersion in both n and k is relatively low.

Table 1. Three layer types are discernable in the TEMs taken from the damselfly's wing membrane; one type exhibits dark greyscale contrast, another type exhibits light greyscale contrast. There are two surface layers exhibiting intermediate greyscale contrast. This table details the parameters associated with the non-dispersive real (n) and imaginary (k) refractive index values that were determined from fitting experimental reflectance data to multilayer theory.

Layer type	n	k
Dark contrast	1.70	0.17
Light contrast	1.56	0.03
Surface layers	1.38	0.00

Using our model as a starting point, we set out to understand the reason for the key physical difference between the structure of the dorsal and ventral DBRs, asking the question "why does only the second layer in each DBR appear to be significantly different?". To this end, we calculated the variation in the system's peak-wavelength of reflection, for different chosen layer thicknesses, by separately changing the thickness of individual layers within each DBR by up to ± 10%. This enabled a detailed examination of the extent to which changes in a particular layer's thickness affected the membrane's overall peak reflected wavelength (Fig. 6). Such changes in thickness of individual layers in either of the dorsal or ventral DBRs will give rise to an increase or decrease in the peak wavelength of reflection and thereby to the perceived colour reflected from the DBR. Figure 6 shows the theoretical results arising from this layer-by-layer thickness variation. It is clear that for both the dorsal and ventral DBR, it is the second-outermost layer (the first dark-contrasted layer from the outer surface visible in TEMs of wing membrane), that gives the greatest change in peak reflected wavelength for a given percentage change in its thickness. In this way, we conclude that for this basic DBR structure, it is the thickness changes in the second layer that most sensitively create colour-changes in the reflected colour-appearance of the wing.

#179627 - $15.00 USD Received 12 Nov 2012; revised 13 Dec 2012; accepted 17 Dec 2012; published 14 Jan 2013

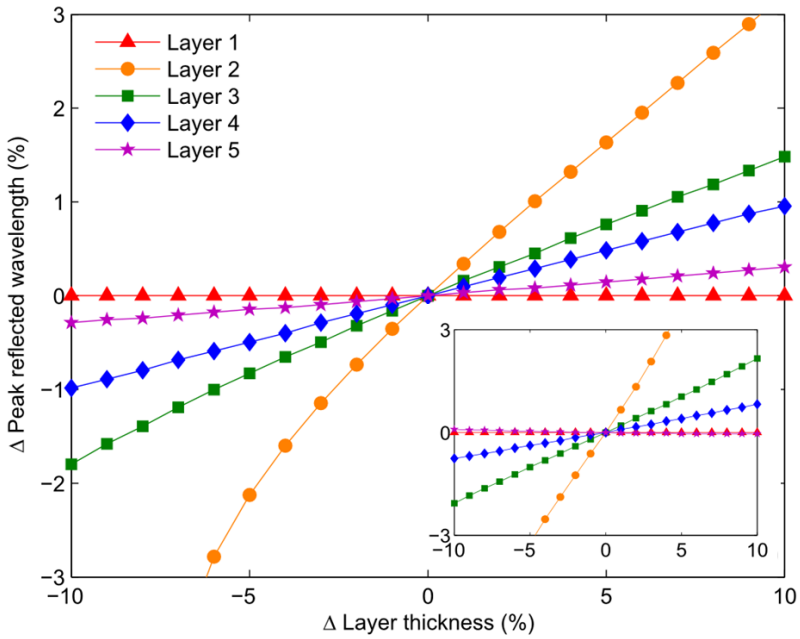

Fig. 6. Graph showing the DBR's sensitivity to change (i.e. the shift in its peak reflected wavelength) due to modifications to individual layer thickness for *M. cyaneipennis'* dorsal DBR. The original, unaltered DBR (the control) is represented by the Δlayer thickness = 0% position. Insert shows the same for *M. cyaneipennis'* ventral DBR.

The underlying optical reason for this is related to the large thickness of layer 2 (more especially its even larger optical thickness) in relation to the thickness of the other layers in each DBR. The DBRs' colour-sensitivity against individual layer-thickness relations, represented by the gradients of the lines shown in Fig. 6 (and inset), scale with the optical thicknesses of the individual layers in each DBR. For comparison, we have analogously modelled the layer thickness sensitivities of an ideal DBR system (in which each layer has the same optical thickness), employing the same refractive indices as those used for the *M. cyaneipennis* DBR models. In that system, all layers returned extremely similar thickness-related colour-sensitivities for the DBR.

3.2 Biological significance

Males of *M. cyaneipennis* differ from those of species of their sister genus, *Neurobasis* (established by sound DNA phylogenetic analysis) [34], in that both fore and hind wing are iridescent and that this occurs on both dorsal and ventral surfaces. In *Neurobasis* species multilayer systems are confined to the upperside of the hindwing with various species reflecting intense green or blue [26]. In *N. chinensis* there are typically 10 optically contrasting layers of cuticle on the wing upperside, and an optically absorbing thick layer on the wing lower side, both of which increase the membrane thickness to 2.0 µm from 1.1 µm measured in the non structurally-coloured-apex of the wing [19]. This significantly increases the mass of the wing and almost certainly affects flight mechanics [26]. In *Neurobasis* species males typically fly with reduced beat amplitude of the hind wings, frequently holding them almost static and supporting themselves with their fore wings, especially when displaying them agonistically to other males or in courtship [35]. To a human observer the iridescent colour is broadcast over a wide angle. By contrast males of *M. cyaneipennis* beat both their wings continually in parallel strokes, producing a series of bright blue flashes from the upperside at a frequency of 8-12 Hz [26]. Underside iridescence is little apparent during normal flight or when the insect is perched with wings folded. However, the undersides of

#179627 - $15.00 USD Received 12 Nov 2012; revised 13 Dec 2012; accepted 17 Dec 2012; published 14 Jan 2013

the wings are clearly presented to perched females during courtship [26]. The gross reflective pattern from *M. cyaneipennis'* wing membrane appears more fractured and sparkling than that of *Neurobasis,* suggesting a much narrower angle of reflectance. This is unlikely to be caused by the degree of rugosity (i.e. rough epicuticular structure on dorsal and ventral wing membrane surfaces that is characteristic of many Odonata and is shown in Fig. 1(a) for *M. cyaneipennis*) since the membrane surfaces of both species exhibit rather similar superficial surface structure. It is more likely caused by the greater degree of variation in relative orientation of wing membrane cells in *M. cyaneipennis* compared to *Neurobasis.* Nevertheless as the wings are presented dynamically to their conspecifics the colours doubtless retain strong semiotic value. It is quite common for calopterygoid damselflies such as *M. cyaneipennis* to possess wing and body ornaments specialised for courtship or territorial display [36]. As the total thickness of the iridescent wing membrane in *M. cyaneipennis* is just 1.69 μm it appears to have achieved a remarkable two-colour signalling system at relatively little cost in terms of gain in wing mass.

4. Conclusions

M. cyaneipennis displays two noticeably different iridescent colours from either side of its hind wings. We have shown these are the result of two DBR structures that are nearly identical except for the thickness of the second layer from each DBR surface. Layer-by-layer modelling, using the block refractive index analysis method, confirms that the thickness variations between individual layers in the dorsal and ventral DBRs are optimised to give the greatest difference in colour-appearance from the smallest variation in thickness. We suggest that selection pressures on the evolution of *M. cyaneipennis* have identified the most developmentally and biomechanically efficient route for significantly modifying the colour of a simple single multilayer system on either side of its wings. This species frequents dappled sun patches on small streams in dense equatorial montane forest. Its unique colouration, together with co-adapted flight style, likely form an effective system for short-range signalling, even in poor illumination.

Acknowledgments

Pete Vukusic acknowledges the financial support of AFOSR grant FA9550-10-1-0020. We thank D.G. Stavenga for critical reading of the manuscript.

#179627 - $15.00 USD Received 12 Nov 2012; revised 13 Dec 2012; accepted 17 Dec 2012; published 14 Jan 2013